Atypical charge redistribution over a charge-transfer monolayer on a metal

2013 New J. Phys. 15 083048

(http://iopscience.iop.org/1367-2630/15/8/083048)

New Journal of Physics
The open access journal for physics

Atypical charge redistribution over a charge-transfer monolayer on a metal

T R Umbach[1], I Fernández-Torrente[1], M Ruby[1], F Schulz[1], C Lotze[1], R Rurali[2], M Persson[3,4], J I Pascual[1,5,6] and K J Franke[1,7]

[1] Institut für Experimentalphysik, Freie Universität Berlin Arnimallee 14, D-14195 Berlin, Germany
[2] Institut de Ciencia de Materials de Barcelona (ICMAB-CSIC), Campus de Bellaterra, E-08193 Bellaterra, Barcelona, Spain
[3] The Surface Science Research Center, The University of Liverpool, Liverpool L69 3BX, UK
[4] Department of Applied Physics, Chalmers University of Technology, SE-412 96 Göteborg, Sweden
[5] CIC nanogune, 20018 Donostia-San Sebastian, and Ikerbasque, Basque Foundation for Science, E-48011 Bilbao, Spain
[6] Ikerbasque, Basque Foundation for Science, E-48011 Bilbao, Spain
E-mail: franke@physik.fu-berlin.de

New Journal of Physics **15** (2013) 083048 (9pp)
Received 21 February 2013
Published 23 August 2013
Online at http://www.njp.org/
doi:10.1088/1367-2630/15/8/083048

Abstract. We report an atypical charge distribution in a highly ordered monolayer of sodium (Na) and tetracyanoquinodimethane (TCNQ) on a Au(111) surface. Na atoms incorporated in the charge-transfer layer donate their 3s electron to the lowest unoccupied orbital of the TCNQ acceptor. A fingerprint of such a TCNQ anion is observed in scanning tunneling spectroscopy as a zero-bias peak characteristic of the Kondo effect. Spatial maps of the Kondo resonance surprisingly reveal that it appears most intense on top of the Na sites. Supported by density functional theory simulations, we interpret this peculiar charge distribution pattern as originating from the extension of the singly occupied molecular orbital beyond the molecular backbone, and

[7] Author to whom any correspondence should be addressed.

cloaking the Na cations. We further suggest that this deformation of molecular orbitals is a consequence of the electrostatic potential landscape of the polar Na–TCNQ layer.

Crystalline thin films of organic compounds are a basic element in future soft-matter electronic devices. An important aspect governing their electronic, optical or magnetic functionality is the distribution of electrons in the valence orbitals of the molecular constituents [1]. Factors like the molecular structure, the electron affinity or the polarizability of the crystalline surrounding determine the extension of electron clouds and, hence, their redistribution throughout the crystalline structure.

Electron redistribution in organic salts is particularly interesting because electron transfer between donor and acceptor species results in a polar lattice of anions and cations. Due to the ionic nature of the bond between donor and acceptor and to electron correlation effects within the homomolecular stacks, the charge is generally assumed to be localized in the molecular sites [2]. In fact, models based on a lattice of point charges have been successfully employed to describe the optical, electronic and transport properties of the organic salts [3, 4]. Charge transfer salts of alkali donors and tetracyanoquinodimethane (TCNQ) acceptors are a particular example of intramolecular electron localization in the acceptor species. The absence of wave function overlap between the frontier orbitals of TCNQ and the alkali cations, and the large electron affinity, keep the unpaired electron localized at the cyano terminations of TCNQ molecules [5, 6].

An intriguing question, which we treat here, is whether the charge localization persists in a monolayer of a charge-transfer salt in contact with a metal surface. Even in the absence of strong bonds, the metal is expected to significantly influence the charge distribution in the ionic layer. Screening of the ionic sites by the metal substrate electrons can favor further charge donation and alter the charge distribution. To probe the extension of valence electrons throughout a molecular layer on a metal surface, Kelvin probe force microscopy (KPFM) has been recently employed [7]. When brought down to the atomic level, this method resolved maps of the electrostatic potential with intramolecular resolution, which could be related to charge redistribution within a molecule on an insulating layer. However, when the polar alkali-molecule layers lie on a metal surface, the KPFM results are more difficult to interpret, since they are influenced by contributions from lattice and surface dipoles. An additional fingerprint of unpaired electrons on a metal surface is the Kondo effect. Here, we probe the spatial distribution of a Kondo resonance by scanning tunneling microscopy (STM) and relate it to a map of the unpaired electron density.

With this method, we resolve an atypical charge redistribution occurring in a monolayer of the charge transfer salt Na–TCNQ deposited on a Au(111) metal surface. The Na atoms donate a full electron to the organic acceptor, and the unpaired electron in a π orbital gives rise to a Kondo resonance in the tunneling spectra measured with a STM [8, 9]. Despite this donation, high resolution spatial maps of the Kondo state reveal a large unpaired electron density on top of the Na cations. Supported by density functional theory (DFT) calculations, this behavior reveals that the hosting orbital extends into the vacuum and covers the Na cation with an electron cloak. The resulting charge rearrangement screens the alkali cations from their exposure to vacuum and is expected to crucially affect the film properties.

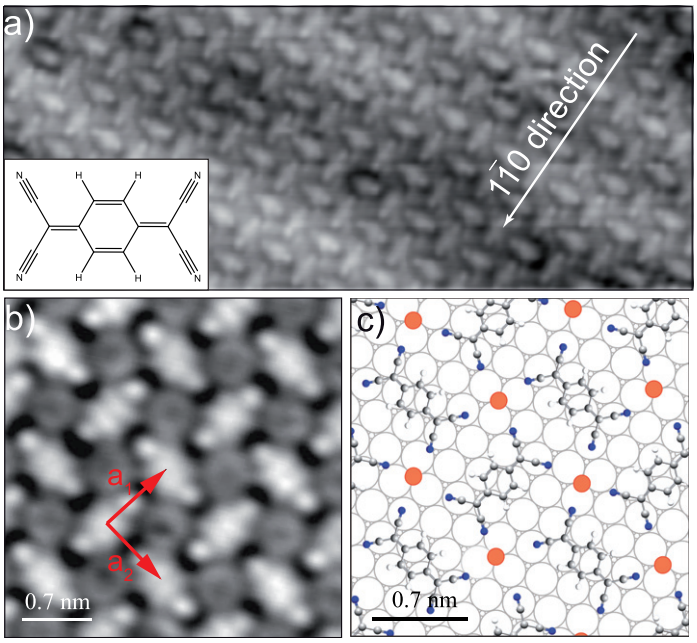

Figure 1. (a) STM topographic image of the mixed Na–TCNQ layer on Au(111) (scanning parameters: $I_t = 110\,\text{pA}$, $V_t = 76\,\text{mV}$). Inset: molecular structure of TCNQ. (b) High resolution image with the windmill structure adopted by TCNQ (scanning parameters: $I_t = 100\,\text{pA}$, $V_t = 100\,\text{mV}$). (c) Structural model of the Na–TCNQ layer on Au(111). The dimensions of the unit cell vectors are $|\vec{a}_1| = |\vec{a}_2| = (0.9 \pm 0.1)\,\text{nm}$. Data analysis was performed with the WSxM software [26].

Our experiments were done in a custom-made STM, under ultra-high vacuum conditions and at a base temperature of 4.8 K. The Au(111) single crystal was cleaned by repeated Ne^+ sputtering and annealing cycles until an atomically flat surface was observed, exhibiting the characteristic Au(111) herringbone reconstruction. TCNQ and Na were sublimated in vacuum (from a Knudsen cell and an alkali metal dispenser from SAES, respectively) onto the sample at 330 K. The sample was then cooled down and transferred into the cold STM.

The sub-monolayer mixture of Na and TCNQ forms highly ordered square-like structures on the Au(111) surface (figure 1). Intra-molecular resolution reveals characteristic nodal plane patterns of the TCNQ orbitals (figure 1(b)). This behavior is an indication of TCNQ species lying flat on the surface. The molecules are arranged with four electrophilic cyano endgroups pointing toward a single site, revealing the inclusion of a Na atom at this site [10]. The resulting structure of the Na–TCNQ domains resemble, in shape and size, the arrangement of Na–TCNQ layers of the bulk compound [11], in contrast to that of the pure TCNQ layer [12]. Thus, the surface seems to play a minor role in the assembly process, as also corroborated by the observation of the intact herringbone reconstruction underneath the mixed layer (figure 1(a)).

The stabilization of a windmill TCNQ structure by the incorporation of alkali atoms is only possible if we consider the different electron affinity character of the two species. In the bulk phase of the Na–TCNQ compound, the Na atoms donate their 3s electron to the electrophilic TCNQ molecule [13], increasing the electron density at the cyano terminations [5].

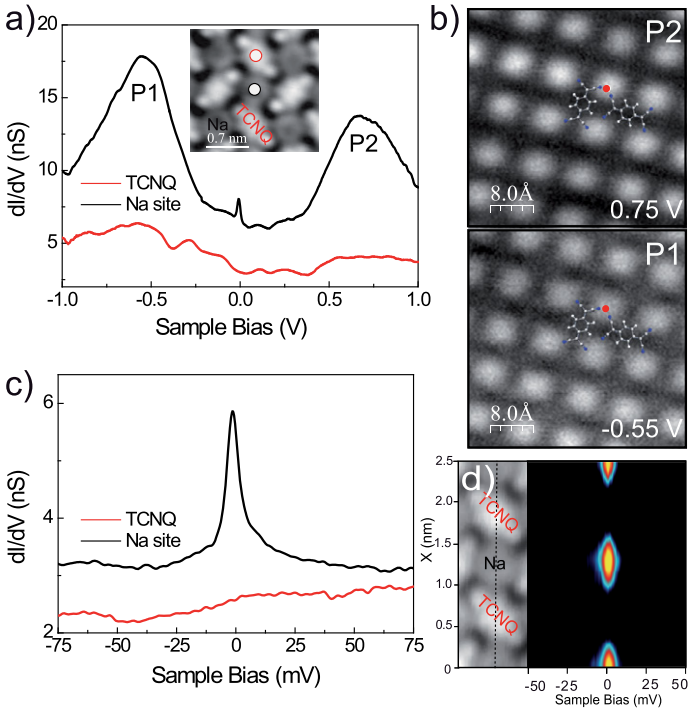

Figure 2. (a) $\mathrm{d}I/\mathrm{d}V$ spectra acquired on two different sites of the alkali-molecular layer ($V_t = 0.1$ V, $I_t = 0.3$ nA, $V_{ac} = 3$ mV rms at 821 Hz). The spectra are vertically offset for clarity. (b) Conductance maps taken at the energies of P1 and P2 resonances. The molecular model shows the localization of the P1 and P2 resonances on top of the Na atom. The maps were taken at constant current ($I_t = 0.5$ nA, $V_{ac} = 12$ mV rms at 877 Hz). (c) High resolution $\mathrm{d}I/\mathrm{d}V$ spectra around E_F on Na and TCNQ sites ($V_t = 100$ mV, $I_t = 2.5$ nA, $V_{ac} = 1$ mV rms at 877 Hz). The spectrum on the Na site shows a narrow zero-bias peak. The spectra are shifted vertically for clarity. (d) Spectral map along the dashed line indicated in the topography image. The maps clearly show the localization of the Kondo resonance on top of Na sites.

The cohesion of the molecular solid is thus due to electrostatic interactions between the Na cation and the radical TCNQ anion. On the gold surface, this picture is likely to persist, albeit screening by the metal substrate electrons may stabilize alternative charge transfer patterns.

To probe the charge redistribution in the Na–TCNQ/Au(111) interface, we compare differential conductance ($\mathrm{d}I/\mathrm{d}V$) spectra on different sites of the layer (figure 2(a)). The spectra measured on top of TCNQ molecules are featureless. In contrast, spectra on Na sites exhibit two broad features centered at -0.55 and 0.7 eV with respect to the Fermi level (E_F), labeled P1 and P2 in figure 2(a), and mapped in figure 2(b). In the spectra on the Na sites (shown in figure 2(c)) we also observe a sharp zero-bias peak (linewidth of 7 ± 1 mV) attributed to the Kondo effect commonly observed in this family of organic salts [14–16]. This peak is a fingerprint of the presence of an unpaired electron on Na sites. A series of spectra along Na atoms and TCNQ molecules (figure 2(d)) reveals that the Kondo resonance is spatially localized solely on the

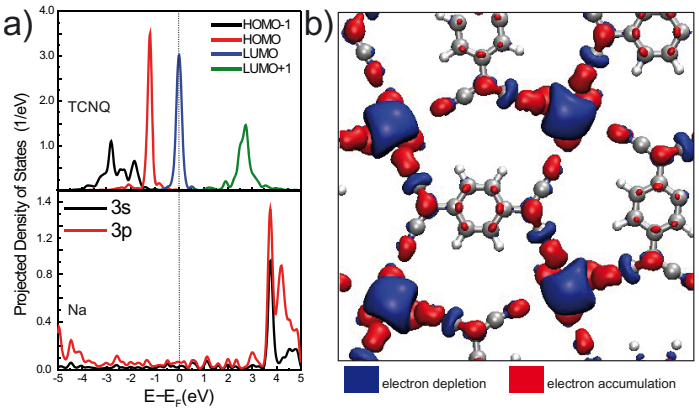

Figure 3. (a) Calculated projected density of states of the Na–TCNQ monolayer on the frontier orbitals of a TCNQ molecule and on the 3s and 3p orbitals of the Na atom. The LUMO-derived state of TCNQ is aligned close to E_F and partially occupied by a single electron. (b) Map of the induced electron density created by incorporation of the Na atom in the TCNQ/Au(111) layer ($n_{\text{induced}} = n_{(\text{Na–TCNQ/Au})} - n_{(\text{TCNQ/Au})} - n_{\text{Na}}$). Blue corresponds to electron depletion and red to electron accumulation, respectively.

Na sites and vanishes on top of TCNQ molecules. The localization of both Kondo resonance and peaks P1 and P2 on Na sites cannot be explained by invoking a simple ionic-like electron transfer from Na to TCNQ, because the resulting closed shell Na cation would have atomic orbitals lying far from the Fermi level and no unpaired electron. To elucidate the origin of such unexpected distribution of the Kondo resonance, we performed DFT calculations using the plane wave Vienna *ab initio* simulation package code [17]. The ion–core interactions and the exchange correlation effects were handled using the projector augmented wave method [18] and the optB86b version of the van der Waals density functional [19], respectively. The Au(111) substrate is represented in a supercell by a four layer slab with a c$(7 \times 4\sqrt{3})$ surface unit cell. The four Na atoms and four TCNQ molecules in the surface unit cell were placed following the structure suggested by experiments with the Na atoms in the hollow site[8,9].

We first confirm that the expected electron transfer from Na to TCNQ species takes place on the Au(111) surface by projecting the total density of states (DOS) of the Na–TCNQ/Au(111) system onto Na and TCNQ orbitals, respectively (figure 3(a)). Na 3s and 3p atomic orbitals are empty and aligned far from the Fermi level, proving the full donation of the Na unpaired electron. The TCNQ lowest unoccupied orbital (LUMO) is pinned at the Fermi level and partially filled, corresponding to a singly occupied molecular orbital (SOMO) resonance. The two resonances arising from hole and electron attachment to the SOMO correspond to the P1 and P2 resonances.

[8] The bottom two layers were held at their bulk positions with a calculated lattice constant of 4.137 Å during the structural relaxations until all forces were less than 0.02 eV Å^{-1}. A plane wave, kinetic energy cut-off of 400 eV was used and the k points in the Brillouin zone were sampled by a $2 \times 2 \times 1$ grid. The vacuum region was 19.6 Å.

[9] After relaxation of the Na–TCNQ structure on the Au(111) surface, a small asymmetry occurs in the bonding of the TCNQ molecules to the Na centers. This is reflected in two types of TCNQ molecules. Their electronic properties are similar. For clarity, we restrict ourselves to the general observations found in both types.

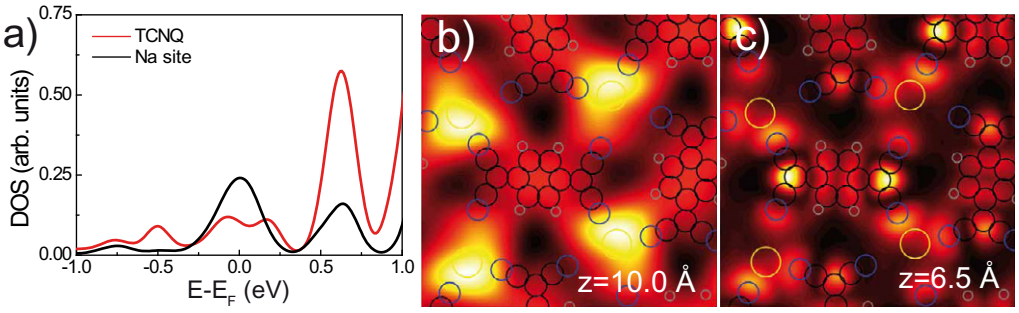

Figure 4. (a) Calculated LDOS at a distance of 10 Å from the surface on top of a Na site and on top of the center of a TCNQ molecule. (b), (c) Maps of the LDOS at E_F, corresponding to the TCNQ SOMO resonance at a distance of 10 and 6.5 Å from the surface, respectively.

The electron rearrangement can be pictured by mapping the induced electron density upon incorporation of Na atoms in the TCNQ/Au(111) system (figure 3(b)). There is a clear electron depletion at the Na sites, and an increased electron density at the cyano terminations of the TCNQ molecules. The empty 3s state of the Na atom and the formation of a SOMO resonance on the TCNQ (figure 3(a)) yield a transfer of ~ 1 electron from donor to acceptor.

The metal substrate is not directly involved in the electron transfer, in agreement with the persisting appearance of the Au(111) herringbone reconstruction and the negligible shift of the Au(111) surface state [10]. Furthermore, the absence of relevant Na states around the Fermi level is significative of a negligible hybridization of Na and TCNQ orbitals, commonly found when transition metals are used instead of alkali atoms [20–22]. Thus, the ionic-like charge transfer appears as the primary source of bonding between Na and TCNQ species, stabilizing the layered structure [20].

At first sight, the formation of an unpaired electron on the TCNQ molecule by electron donation from the Na atom contradicts the observation of a Kondo resonance centered at Na sites. To unravel this apparent contradiction, we compare in figure 4 the local density of states (LDOS) around E_F at different locations on the Na–TCNQ layer. We explore first the LDOS at a distance of 10 Å from the surface, representing the case of imaging at low tunneling conductance (figure 4(a)). We find a peak centered at E_F that has a larger weight on top of the Na sites than on the TCNQ. This corresponds to the TCNQ SOMO resonance close to E_F giving rise to the Kondo effect. This corroborates the experimental finding of a larger weight of the Kondo resonance on top of the Na sites than on the TCNQ molecule.

The origin of the unexpected Kondo resonance is due to the particular spatial rearrangement of molecular states in the presence of the alkali atom. At 10 Å over the surface (figure 4(b)) the TCNQ SOMO resonance has dominant weight on top of the Na cation. At a smaller distance from the surface (e.g. at 6.5 Å in figure 4(c)), the SOMO recovers the characteristic nodal plane structure of the unperturbed LUMO of TCNQ. This characteristic distance dependence of the localization of the SOMO is reflected in differential conductance maps measured at the energy of resonance P2. Peaks P1 and P2 correspond to hole and electron attachment into the SOMO state, so that their distribution can be correlated with the DOS maps in figure 5. In figure 5 we compare three (constant current) $\mathrm{d}I/\mathrm{d}V$ maps measured with setpoint currents of 30, 300 and 3000 pA. The map recorded with $I_t = 30$ pA shows a pronounced intensity on top of the

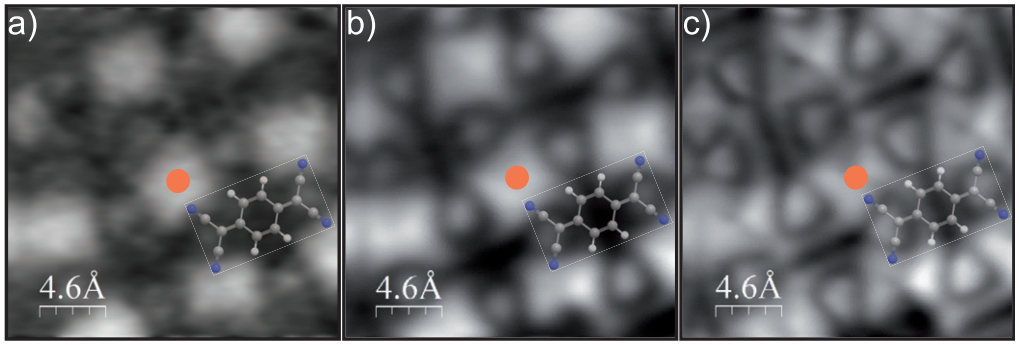

Figure 5. Constant current dI/dV maps at the resonance P2 (550 mV) for different current set points $I_t = 30$, 300 and 3000 pA, respectively ($V_{ac} = 5$ mV rms at 821 Hz).

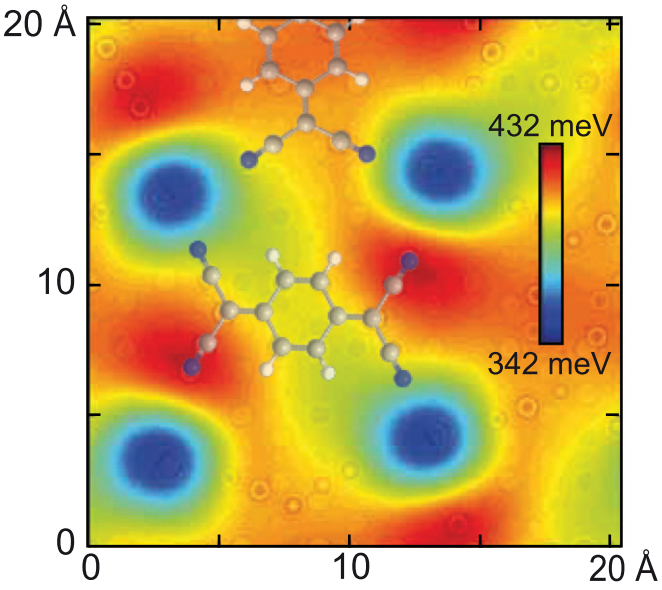

Figure 6. Map of the electrostatic potential energy felt by an electron at a distance of 8 Å from the Au(111) top most layer. The color scale ranges from 342 meV (blue) to 432 meV (red).

Na sites, similar to the simulated DOS at large tip-sample distance[10]. At a tunneling current of $I_t = 3000$ pA, the molecular nodal planes are already distinguishable. This qualitatively resembles the DOS simulation of the SOMO resonance at small tip–sample distance. Hence, the peculiar localization of the Kondo resonance is a fingerprint of a charge redistribution, with the SOMO of TCNQ anions extending to cloak the Na cation.

The positive charge of the Na ion is responsible for the peculiar distortion in the spatial extension of the TCNQ SOMO by locally modifying the electrostatic potential landscape.

[10] The simulated local density of states at a certain distance does not simply reflect the real tip–sample distance. According to the Tersoff–Hamann theory, the former distance includes the tip apex radius [23]. A direct comparison between experiment and theory of absolute distances is thus intricate.

Figure 6 shows the electrostatic potential energy map for an electron, calculated at a distance of 8 Å from the outermost Au surface layer. On top of the Na cations, the electrostatic potential landscape for electrons shows a ~ 90 meV local minimum, representing a large attractive interaction for the electrons above the Na cation. In the absence of a second layer this attraction favors the three-dimensional deformation of the TCNQ SOMO over the Na ion. The effect of this inhomogeneous potential landscape on the resulting orbital rearrangement occurs also for the free-standing layer in the same geometry as for the adsorbed layer and is not an effect of the metal substrate.

An intriguing result is that the Kondo effect persists for molecular states on top of the Na cation. The Kondo temperature estimated from the experimentally determined values of resonances P1 and P2 (line width Γ and separation U [24]) is consistent with the width of the zero-bias resonance in figure 2(c) and is similar to the Kondo temperature for other TCNQ based charge transfer salts [14, 16]. This shows that the presence of the Na cation underneath the SOMO resonance clearly has no effect on the nature of the Kondo screening. We ascribe this to the absence of any Na-related state in a wide window of energy around E_F. On the other hand, this further corroborates that the Kondo screening arises from a single orbital and with a single screening channel [25]. In summary, mapping of the Kondo resonance reveals a highly peculiar charge redistribution in the monolayer of the charge transfer salt Na–TCNQ. The observation of the Kondo effect on top of the cation is due to its cloaking by the singly occupied molecular orbital of the neighboring molecule.

Acknowledgments

We thank Martina Corso for fruitful discussions. We gratefully acknowledge funding by the DFG through grant numbers FR 2726/1 and Sfb 658. MP is grateful for funding from VR, the EU project ARTIST and the Leverhulme Trust (F/00 025/AQ) and the allocation of computer resources at HECToR through the membership in the materials chemistry consortium funded by EPSRC (EP/F067496) and at Lindgren, PDC through SNIC. RR acknowledges funding under contract numbers FIS2012-37549-C05-05 and CSD2007-00041.

References

[1] Kumai R, Okimoto Y and Tokura Y 1999 *Science* **284** 1645–7
[2] Topham B J and Soos Z G 2011 *Phys. Rev.* B **84** 165405
[3] Torrance J B and Silverman B D 1977 *Phys. Rev.* B **15** 788–801
[4] Soos Z G 1974 *Annu. Rev. Phys. Chem.* **25** 121–53
[5] Jonkman H T and Kommandeur J 1972 *Chem. Phys. Lett.* **15** 496–9
[6] Vegter J G and Kommandeur J 1974 *Phys. Rev.* B **9** 5150–4
[7] Mohn F, Gross L, Moll N and Meyer G 2012 *Nature Nano* **7** 227–31
[8] Li J, Schneider W-D, Berndt R and Delley B 1998 *Phys. Rev. Lett.* **80** 2893–6
[9] Madhavan V, Chen W, Jamneala T, Crommie M F and Wingreen N S 1998 *Science* **280** 567–9
[10] Wäckerlin C, Iacovita C, Chylarecka D, Fesser P, Jung T A and Ballav N 2011 *Chem. Commun.* **47** 9146–8
[11] Konno M and Saito Y 1974 *Acta Crystallogr.* B **30** 1294–9
Konno M and Saito Y 1975 *Acta Crystallogr.* B **31** 2007–12
[12] Fernández-Torrente I, Franke K J and Pascual J I 2008 *Int. J. Mass Spectrom.* **277** 269–73
[13] Melby L R, Harder R J, Hertler W R, Mahler W, Benson R E and Mochel W E 1962 *J. Am. Chem. Soc.* **84** 3374–87

[14] Fernández-Torrente I, Franke K J and Pascual J I 2008 *Phys. Rev. Lett.* **101** 217203
[15] Choi T, Bedwani S, Rochefort A, Chen C-Y, Epstein A J and Gupta J A 2010 *Nano Lett.* **10** 4175–80
[16] Fernández-Torrente I, Kreikemeyer-Lorenzo D, Stróżecka A, Franke K J and Pascual J I 2012 *Phys. Rev. Lett.* **108** 036801
[17] Kresse G and Furthmüller J 1996 *Phys. Rev.* B **54** 11169–86
[18] Kresse G and Joubert D 1999 *Phys. Rev.* B **59** 1758–75
[19] Klimeš J, Bowler D R and Michaelides A 2011 *Phys. Rev.* B **83** 195131
[20] Abdurakhmanova N, Floris A, Tseng T-C, Comisso A, Stepanow S, deVita A and Kern K 2012 *Nature Commun.* **3** 940
[21] Faraggi M N, Jiang N, Gonzalez-Lakunza N, Langner A, Stepanow S, Kern K and Arnau A 2012 *J. Phys. Chem.* C **116** 24558–65
[22] Jono R, Fujisawa J-I, Segawa H and Yamashita K 2011 *J. Phys. Chem. Lett.* **2** 1167–70
[23] Olsson F E, Persson M and Lorente N 2003 *Surf. Sci. Lett.* **522** L27
[24] Hewson A C 1997 *The Kondo Problem to Heavy Fermions* (Cambridge: Cambridge University Press)
[25] Romero M and Aligia A A 2011 *Phys. Rev.* B **83** 155423
[26] Horcas I, Fernandez R, Gomez-Rodriguez J M, Colchero J, Gomez-Herrero J and Baro A M 2007 *Rev. Sci. Instrum.* **78** 013705